(NASA-TM-84991) SIMULATING SPATIAL AND TEMPORAL VARIATION OF CORN CANOPY TEMPERATURE DURING AN IRRIGATION CYCLE (NASA) 41 p HC A03/MF A01 CSCL 02C

N83-22694

Unclas G3/43 09956

NASA

Technical Memorandum 84991

SIMULATING SPATIAL AND TEMPORAL VARIATION OF CORN CANOPY TEMPERATURE DURING AN IRRIGATION CYCLE

B.J. Choudhury and C.A. Federer

FEBRUARY 1983

National Aeronautics and Space Administration

Goddard Space Flight Center
Greenbelt, Maryland 20771

TM 84991

SIMULATING SPATIAL AND TEMPORAL VARIATION OF CORN CANOPY TEMPERATURE DURING AN IRRIGATION CYCLE

Bhaskar J. Choudhury
Hydrological Sciences Branch
Goddard Space Flight Center
Greenbelt, MD 20771

C. Anthony Federer
U.S. Forest Service
Northeastern Forest Experiment Station
Durham, NH 03824

February 1983

GODDARD SPACE FLIGHT CENTER
Greenbelt, Maryland

SIMULATING SPATIAL AND TEMPORAL VARIATION OF CORN CANOPY TEMPERATURE DURING AN IRRIGATION CYCLE

ABSTRACT

The canopy-air temperature difference (δT) may provide an index for scheduling irrigation. Combining the Monteith transpiration equation with both uptake from a single-layered root zone and change in internal storage of the plant, we have explicitly solved the continuity equation for water flux in the soil-plant-atmosphere system. Using appropriate parameters for corn (*Zea mays* L.) the model indicates that both daily total transpiration and soil-induced depression of plant water potential may be inferred from mid-day δT. For the soil-plant-weather data used in the simulation, either a mid-day spatial variability of about 0.8K in canopy temperatures or a field-averaged δT of 2 to 4K might be a suitable criterion for irrigation scheduling.

INTRODUCTION

Irrigation scheduling should maximize the benefit of each unit of irrigation water. Recently Jackson (1982) argued that direct observation of some plant factor should be a superior approach to optimizing irrigation than use of soil or meteorologic factors. The plant factors that have been studied as indicators of plant stress are leaf water potential, stomatal resistance, leaf temperature, and canopy temperature. The leaf-based measurements (potential, resistance, and leaf temperature) are time consuming when fields of the size of hectare or larger are to be sampled to obtain a representative value. Therefore, according to Jackson (1982), the most promising approach to irrigation scheduling would be measurements of canopy temperature using infrared radiometers. Furthermore, identification of crop stress using infrared radiometers can be done at large scale using spaceborne sensors.

Canopy temperature represents an integrated response of a crop to prevailing weather and soil water conditions. In the absence of any soil water deficit, diurnal and day-to-day variations in the canopy temperature would be due to the weather parameters (insolation, wind speed, air and dew point temperatures). As transpiration becomes limited by depleting soil water the canopy temperature increases with respect to air temperature, so that the reduced transpiration is balanced by increased heat loss. In a field study of irrigation scheduling for corn (*Zea mays* L.) using infrared thermometers, Clawson and Blad (1982) showed that both canopy temperature and its spatial variation can be used effectively to reduce irrigation water without affecting yield.

The plant, soil, and atmospheric factors that control plant water stress and leaf-air temperature difference are fairly well-known and can be mathematically expressed. Therefore, simulation provides a way to examine crop behavior without the labor and uncontrolled aspects of field experiments.

In this paper we develop a simulation model for canopy-air temperature difference for a corn crop and use it to study temporal and spatial variation of the temperature difference with respect

to irrigation. Choudhury (1983 a,b) solved Monteith's (1965) and van den Honert's (1948) equations for transpiration and tested the results against Idso's (1982) data for unstressed corn and soybeans (*Glycine max* L.) on clear days. The continuity equation for water flux in the soil-plant-atmosphere system is solved by expressing the stomatal resistance and the rate of plant tissue water loss in terms of a plant water potential (Federer, 1979). We have also added the dynamics of root-zone soil water following Feddes and Rijtema (1972), and the increase in flow resistance in a drying plant (Boyer, 1971; Nulsen and Thurtell, 1978). The model currently ignores soil evaporation. Dynamic equations then show the progression of soil water and plant water storage and their effect on canopy temperature through the energy balance equation.

By examining the temporal variation of canopy-air temperature difference during drying we determine if it can be used for irrigation scheduling. We also simulate expected variation of canopy temperature across a field to determine its effect on scheduling.

DESCRIPTION OF THE MODEL

Vapor Phase

For transpirational flux, E_A, (m/s), we use Monteith's (1981) modification of Monteith's (1965) combination equation. This modification accounts for the dependence of net radiation on the canopy temperature by defining an effective boundary-layer resistance.

$$E_A = \frac{\Delta R_{no} + C_p \rho_a (e_a^* - e_a)/r_t}{L_V [\Delta + \gamma (r_a + r_c)/r_t]} \qquad (1)$$

where R_{no} is the net radiation flux absorbed by the canopy if the canopy surface were at air temperature (W m^{-2}), e_a^* and e_a are, respectively, the saturated vapor pressure (kPa) at air and dew point temperature, Δ is the slope of saturated vapor pressure at the air temperature (kPa K^{-1}), C_p and ρ_a are, respectively, the heat capacity (J kg^{-1} K^{-1}) and density (kg m^{-3}) of air, γ is the psychrometric constant (kPa K^{-1}), L_v is the latent heat of vaporization (J m^{-3}), r_c is the canopy resistance (s m^{-1}), and r_t is the effective boundary-layer resistance for heat and longwave radiative transfer (s m^{-1}), given by Monteith (1981) as

$$\frac{1}{r_{eff}} = \frac{1}{r_a} + \frac{1}{\left(\frac{C_p \rho_a}{4 \epsilon_c \sigma T_a^3}\right)} \tag{2}$$

where ϵ_c is the canopy emissivity, σ is the Stefan-Boltzman constant, T_a is the air temperature and r_a is the usual boundary-layer resistance (s m^{-1}), calculated according to Grace (1977) for corn

$$r_a = \frac{75}{LAI\ U^{1/2}} \tag{3}$$

where LAI is the leaf area index and U is the wind speed (m s^{-1}). The net radiation at the top of the canopy is calculated from global insolation (S, W m^{-2}), albedo (α), longwave emissivities of canopy (ϵ_c) and air (ϵ_a) (Idso, 1981) and air temperature as

$$R_{ni} = (1 - \alpha)\, S + (\epsilon_a - \epsilon_c)\, \sigma T_a^4 \tag{4}$$

From the observed (Impens and Lemeur, 1969) extinction coefficient of net radiation in a corn canopy, the absorbed net radiation is

$$R_{no} = R_{ni}\, [1 - \exp\{0.055\ LAI^2 - 0.622\ LAI\}] \tag{5}$$

The canopy resistance depends most strongly upon leaf-water potential and global insolation (Kramer, 1969). From the observed insolation dependence by Uchijima (1976) and leaf-water potential dependence by Reicosky and Lambert (1978) we have calculated the canopy resistance from

$$r_c = \frac{1.4 \times 10^4}{LAI\ (\psi - \psi_c)} \left[1 + \frac{175}{S + 10}\right] \tag{6}$$

where ψ is the plant water potential (m) and ψ_c is the critical potential for stomatal closure.

Liquid Phase

The rate of change of plant water storage (E_T) is modeled according to Federer (1979). Milne et al. (1983) recently justified this approach for trees. The stored water, Q (mm), in the plant is assumed to be at a potential ψ_q that differs from the plant water potential, ψ, which

controls stomatal closure and water flux through the plant. The stored water is considered to be isolated from the transpiration stream by a resistance R_q (s). Thus,

$$E_T = \frac{\psi_q - \psi}{R_q} \tag{7}$$

Federer (1979) modeled ψ_q as a linear function of Q

$$\psi_q = \psi_c \left[1 - \frac{Q}{Q_o}\right] \tag{8}$$

where Q_o is the maximum storage. However, for the current model we tried to get a more realistic function. Presumably the stored water is in living cells, primarily in the plant stem; but we are not aware of $\psi_q - Q$ relations of such cells. As the best alternative we assume that the relation of leaf water content to leaf water potential applies also to storage cells in the stem. To observations of Reicosky and Lambert (1978) for corn we fitted a bi-linear equation (Fig. 1)

$$\psi_q = -450\ Xf - (131\ X + 84)\ (1-f) \tag{9}$$

where

$$X = 1 - \frac{Q}{Q_o}$$

and

$$f = \frac{1}{1 + 6093\ X^5}$$

The rate of water extraction by plant roots (E_s in m s^{-1}) is calculated from van den Honert's 1948 equation

$$E_s = \frac{\psi_s - \psi}{R_s + R_p} \tag{10}$$

where ψ_s is the soil water potential (m), and R_s and R_p are, respectively, the resistances for water flow within soil to the root surface and from the root surface to leaf stomata.

The soil resistance is calculated from an empirical form of the Gardner – Cowan equation given by Feddes and Rijtema (1972)

$$R_s = \frac{0.0013}{Z_{eff}\, K(\psi_s)} \tag{11}$$

where Z_{eff} is the effective root depth (m) and $K(\psi_s)$ is the unsaturated hydraulic conductivity of soil (m s^{-1}), given in the parametric form by Campbell (1974) as

$$K(\psi_s) = K_s \left[\frac{\psi_{sat}}{\psi_s}\right]^{2 + 3/b} \tag{12}$$

where the parameters K_s, ψ_{sat} and b for different soil texture classes can be found in Clapp and Hornberger (1978).

The plant resistance is calculated as the ratio of root resistance per unit length r_r (s m^{-1}) and root length per unit area L_T (m^{-1}) as

$$R_p = \frac{r_r}{L_T} \tag{13}$$

Boyer (1971) and Nulsen and Thurtell (1978) observed that when a corn plant is subjected to stress its root resistance increases. Because shrinkage of roots resulting from a loss of tissue water is thought to increase the resistance (Vaadia et al., 1961), we have modeled the stress induced changes in the plant resistance as

$$r_r = r_{ro}\left\{[1 - f]\, X^{1/2} + 1\right\} \tag{14}$$

where r_{ro} is the unstressed root resistance, and f and X are tissue water dependent quantities defined in Equation (9). The functional form is chosen quite arbitrarily; however, Equation (14) recognizes a non-linear dependence of the resistance on the storage potential, ψ_q, and on the duration of stress noted by Nulsen and Thurtell (1978), as reflected in the amount of storage.

Equations of Continuity and Energy Balance

The continuity equation for water flux in the soil-plant-atmosphere system is

$$E_A = E_S + E_T \tag{15}$$

where the fluxes are defined by Equations (1), (7) and (10).

The energy balance equation is

$$T_c - T_a = [R_n - L_V E_A] (r_{eff}/C_p \rho_a) \tag{16}$$

where T_c is the canopy temperature.

Dynamic Equations

The dynamics of plant storage water Q (mm) follows from Federer (1979)

$$\frac{dQ}{dt} = -10^3 E_T \tag{17}$$

and the dynamics of root-zone soil water potential ψ_s comes from integrating the diffusion equation for moisture flux

$$Z_{eff} V(\psi_s) \frac{d\psi_s}{dt} = -E_s - K(\psi_s) \tag{18}$$

where the soil capacitance $V(\psi_s)$ is given by (using Clapp and Hornberger's (1978) equation relating volumetric moisture to the matric potential)

$$V(\psi_s) = \left(\frac{d\theta}{d\psi_s}\right) = -\frac{\theta_s}{b\,\psi_{sat}} \left(\frac{\psi_{sat}}{\psi_s}\right)^{1+1/b} \tag{19}$$

and θ_s and ψ_{sat} are, respectively, the saturation volumetric moisture and matric potential.

Method of Solution

Substituting (1), (6), (7), and (10) into (15) yields a quadratic equation in leaf water potential ψ, which has the solution

$$\psi = [-B + (B^2 - 4AC)^{1/2}]/(2A) \tag{20}$$

where

$$A = (\Delta + \gamma^*)\, r_t \left[\frac{1}{R_s + R_p} + \frac{1}{R_q}\right]$$

$$B = (\Delta + \gamma^*)\, r_t\, (E_o - \psi_e) - (\alpha - \gamma r')\left[\frac{1}{R_s + R_p} + \frac{1}{R_q}\right]$$

$$C = (\alpha - \gamma r')\, \psi_c - E_o \alpha$$

$$\gamma^* = \gamma\, r_a / r_t$$

$$E_o = \frac{\Delta\, R_{no} + C_p \rho_a\, (e_a^* - e_a)/r_t}{L_V\, [\Delta + \gamma^*]} \qquad (21)$$

$$\psi_e = \frac{\psi_s}{R_s + R_p} + \frac{\psi_q}{R_q}$$

$$\alpha = (\Delta + \gamma^*)\, r_t\, \psi_c$$

$$r' = \frac{1.4 \times 10^4}{LAI}\, [1 + 175/(S + 10)]$$

For any given set of weather variables (insolation, wind speed, and air and dew point temperatures), plant properties (leaf area index, storage resistance, root depth and root length per unit area) and soil texture parameters (b, K_s, ψ_s and θ_s) one can calculate the plant potential when the plant storage Q and the soil water potential ψ_s are specified. Diurnal weather variables determine the evaporative demand (E_o) and Equations (17) and (18) give the diurnal variation of ψ_s and Q.

The numerical method used for the solution of Equations (17) and (18) is the Douglas-Jones implicit linearization (Douglas and Jones, 1963). If we define functions $F_1\ (\psi_s, Q, \psi)$ and $F_2\ (\psi_s, Q, \psi)$ as

$$F_1\ (\psi_s, Q, \psi) = \frac{-1}{Z_{eff}\, V(\psi_s)} \left[\frac{\psi_s - \psi}{R_s + R_p} + K(\psi_s)\right] \qquad (21)$$

$$F_2\ (\psi_s, Q, \psi) = -10^3 \left[\frac{\psi_q - \psi}{R_q}\right] \qquad (22)$$

then from the starting values ψ_s° and Q° one obtains the new values ψ_s^n and Q^n after time Δt in two steps; the intermediate step,

$$\tilde{\psi}_s = \psi_s^\circ + \frac{\Delta t}{2} F_1 (\psi_s^\circ, Q^\circ, \psi^\circ) \tag{23}$$

$$\tilde{Q} = Q^\circ + \frac{\Delta t}{2} F_2 (\psi_s^\circ, Q^\circ, \psi^\circ) \tag{24}$$

and the final step

$$\psi_s^n = \psi_s^\circ + \Delta t\, F_1 (\tilde{\psi}_s, \tilde{Q}, \tilde{\psi}) \tag{25}$$

$$Q^n = Q^\circ + \Delta t\, F_2 (\tilde{\psi}_s, \tilde{Q}, \tilde{\psi}) \tag{26}$$

where ψ° and ψ are obtained from Equation (19) using, respectively, (ψ_s°, Q°) and $(\tilde{\psi}_s, \tilde{Q})$.

Knowing ψ from Equation (20) one can calculate the transpirational flux E_A from Equations (6) and (1). The canopy temperature T_c then follows from Equation (16).

METHODS

Parameter Selection

Reicosky et al. (1975) and Reicosky and Lambert (1978) provide concurrent field data for microclimate and leaf water potential for corn crops. We chose data from June 1 and June 6 in Reicosky et al. (1975) and Day 167 in Reicosky and Lambert (1978) for testing and running our model. Effective rooting depth (Z_{eff}) for these crops was 0.3 m; the leaf area index (LAI) was 3.5 on June 1, 3.6 on June 6, and 4.2 on Day 167. We assume albedo (α) is 0.22, canopy emissivity (ϵ_c) is 0.97, and critical potential for stomatal closure (ψ_c) is −215 m. For unstressed root resistance (r_{ro}) we take Newman's (1973) value for detopped corn, 4×10^{12} s m^{-1}. From wet and

dry biomass data of corn (Wang et al., 1982) we estimate the maximum plant water storage (Q_o) is 2 mm.

From Clapp and Hornberger (1978) we chose soil parameters for a sandy loam soil: $b = 4.9$, $\theta_s = 0.435$, $\psi_{sat} = -0.22$ m, $K_s = 3.5 \times 10^{-5}$ m s^{-1}.

We chose root length per unit area (L_T) and storage resistance (R_q) as the values that best fit the model leaf water potential to the field data (assuming midnight soil water potential of -0.6 m): (L_T, R_q) values are (5×10^3, 4×10^{10}) for June 1, (4×10^3, 4×10^{10}) for June 6, and (5×10^3, 4×10^9) for Day 167. Good agreements shown in Fig. 2 provide some confidence in the simulation model, although they do not provide an *ab initio* verification. A sensitivity study, in which the microclimatic data are varied without changing the crop parameters or varying the crop parameters without changing the microclimate, is not done in this paper.

Field-Averaged Drying Cycle and Irrigation

Starting with a mid-night soil water potential of -0.6 m we simulated soil drying for ten days with soil, crop, and climate data of June 1, June 6, and Day 167. This ten-day drying period is referred to below as the drying cycle. Following this drying cycle a simulated irrigation was executed by setting the soil water potential to -0.6 m on the 0100 hour of the eleventh day of simulation. A second ten-day drying period was then simulated.

Spatial Variation

The spatial variation of soil hydraulic properties is assumed to be described by scaling theory (Philip, 1981). According to this theory stochastic variation of saturated conductivity and potential are described by the equations

$$K_s = t^2 \bar{K}_s \tag{27}$$

$$\psi_{mt} = \bar{\psi}_{mt}/t \tag{28}$$

where $\bar{K}_s$ and $\bar{\psi}_{mt}$ are the field averaged values and the scaling parameter t is a random number. We assumed t is a log-normally distributed random number with mean −0.139 and standard deviation 0.511, after Warrick et al. (1977) for Panoche soil. Ten random scaling parameter values were generated, and for each of the ten sets of hydraulic parameters and each of the three test days we simulated a ten-day drying cycle.

We also considered spatial variation of applied irrigation water. After each of the above drying cycles the amount of applied water was generated stochastically by assuming a uniform distribution with mean equal to the amount of water depleted from the root-zone and a coefficient of variation of 0.1. The choice of the coefficient of variation is according to the observations of Clawson and Blad (1982) for a sprinkler irrigated field. Following irrigation, at 0100 hour, we simulated a second ten-day drying cycle. This sequence of ten drying cycles consider spatial variability of applied irrigation water in addition to the soil hydraulic heterogeniety.

SIMULATION RESULTS AND DISCUSSION

Field-Averaged Results

For all three data sets the canopy temperature at 1300 hour increases fairly slowly at the initial stages of soil drying, then the later increase fairly rapidly (Fig. 3). This trend in canopy temperature is consistent with the observations of Clawson and Blad (1982) who had noted that in sandy soils once stress develops, it progresses fairly rapidly. The diurnal trends of canopy-air temperature differences are shown in Fig. 4.

The canopy temperatures do not return to their original unstressed values after irrigation (Fig. 3). This is consistent with the observations of Jackson et al. (1981). The canopy temperatures continue to decrease for a few days after irrigation before beginning to increase again as the soil continues to dry. This trend in the simulation appears because with irrigation, the incurred

loss of plant tissue water during the drying period begins to get restored by the soil. Due to continued soil drying, however, a complete restoration of the plant tissue water does not occur; and, therefore, the canopy temperatures never return to their original (Day 1) unstressed values. It was found that when irrigation is done after 5 or 6 days of drying, then the canopy temperatures do return to values close to the day 1 of simulation. The leaf water potentials and stomatal resistances also show a recovery period of a few days after irrigation (Fig. 5). Such a lag in the recovery of leaf water potentials has been observed for several crops (Kramer, 1969). The rate of recovery of the leaf water potential is more rapid on high evaporative demand day (Day, 167) than on low evaporative demand days (June 1).

The recovery lag suggests that if the stress history of a crop is not known, it may not be possible to infer unambiguously irrigation needs from measuring canopy temperature, leaf water potential or stomatal resistances. For example, Figure 3a shows that day 1 and day 11 have almost identical "well-watered" soil water potentials, but the canopy-air temperature difference differs by about 0.8K. Plant storage, Q, recovers slowly both because of its own resistance R_q, and because the root resistance r_r depends on Q. Consequently the plant may take one to several days to respond to changes in soil water.

Clark and Hiler (1973) compared leaf water potential, stomatal resistance and leaf-air temperature difference of well-watered and water-stressed peas in order to determine the most suitable crop water stress indicator. They concluded that the leaf water potential was more responsive to changes in plant water status. The relationship of the leaf water potential to the soil water potential and the canopy-air temperature difference are shown in Figures 6 and 7. The relationship between the two potentials is essentially linear, for any particular day, down to a soil water potential of about −60 m, below which the plant potential decreases less rapidly (Fig. 6). A linear relationship between the two potentials has been observed by Shinn and Lemon (1968), Ehling et al. (1968) and Brady et al. (1974), among others. From Figure 7 one would conclude that if leaf water potential

is a good indicator of crop water status, so should be the canopy-air temperature difference. However, when simulation results for all 3 days are composed to form one "data" set, it is difficult to see how either the leaf water potential or the canopy-air temperature difference could be a reliable indicator of irrigation needs. In Fig. 5 a leaf water potential of −175 m would correspond to a soil water potential of about −65 m for June 1, but the same leaf water potential for Day 167 corresponds to a soil water potential of about −20 m. Similarly, from Figs. 3a and 3b we see that a canopy-air temperature difference of 3.5K corresponds to a soil water potential of −45 m for June 1, and −70 m for Day 167.

The atmospheric variability significantly affects both the leaf water potential (ψ) and the canopy-air temperature difference δT (Idso et al., 1981; Jackson et al., 1981). At high soil water potentials if we neglect the plant storage change and the soil resistance for water flow to the root surface, then equations (10), (15), and (16) lead to

$$\delta T^{o} = [R_n + \frac{L_v \psi^{o}}{R_p}] (\frac{r_t}{C_p \rho_a}) \tag{29}$$

where the superscript o is used to indicate high soil water potentials (the day 1 values are assumed). Idso (1982) has shown that δT^{o} is a linear function of atmospheric vapor pressure deficit, and that it is relatively insensitive to all other weather parameters. Then equation (29) shows that ψ^{o} will also be strongly affected by the atmospheric vapor pressure deficit, through a linear relationship. Observations of Idso et al. (1981) confirm such a linear relationship. Jackson et al. (1981) defined a crop water stress index (CWSI),

$$CWSI = \frac{\delta T - \delta T^{o}}{\left(\frac{R_{no} r_t}{C_p \rho_a}\right) - \delta T^{o}} \tag{30}$$

to normalize weather dependent variability of canopy temperature. We can define an analogous normalization for the plant water potential, a plant water stress index (PWSI), as

$$PWSI = \frac{\psi - \psi^{o}}{\psi_{c} - \psi^{o}} \tag{31}$$

where ψ_c is the critical potential for stomatal closure. Figure 8 shows that PWSI normalizes for the atmospheric variability and that the soil water information can be inferred more-or-less unambiguously via this index. The relationship between PWSI and CWSI is shown in Figure 9. If radiometric remote sensing is used to calculate a CWSI (Jackson et al., 1981) then one can also obtain a PWSI and hence, the soil water potential.

The concept of using aircraft and space-borne radiometric data to predict crop water requirements for large areas has been investigated by Bartholic et al. (1972), Schmer and Werner (1974) and Jackson et al. (1977), among others. One aspect of this investigation has been to calculate large area daily evapotranspiration (ET) from one-time-of-day measurement of ground temperature. Jackson et al. (1977) observed a significant linear relationship between daily ET and post noon canopy-air temperature difference for wheat. The present simulation shows that for individual days the daily total transpiration is almost linearly related to the 1300 hour canopy-air temperature difference, and the results for the 3 days taken together may also be approximated by a linear relationship (Figure 10). Comparison of these simulation results with the observations of Jackson et al. (1977) indicates that these linear relationships would at least be crop-specific, since for wheat a canopy-air temperature difference of 2K corresponded to an ET of about 3 mm, whereas we simulate 6 mm for corn. The validity of the present simulation results remains to be confirmed by observations.

Spatial Variability

The range of canopy temperatures (CTV) at the 1300 hour of each day of the drying period are shown in Figures 11a and b. The results in Figure 11a are from the first drying cycle which considered soil hydraulic heterogeniety, and in Figure 11b from the second drying cycle which started following the above drying cycle by stochastically replenishing the amount of depleted soil

water from the root-zone. The simulated steep increase in CTV after the first several days of drying is fully consistent with the observations of Clawson and Blad (1982) and supports their contention that CTV can be used very effectively for triggering irrigation. In Clawson and Blad's field experiment, irrigation was triggered at CTV = 0.8, and we see in Figure 11a and b that this occurs first for Day 167, then June 1 and finally June 6. This arrangement of days follows the daily total transpiration (Figure 10), and hence the rate of soil drying. The onset of CTV = 0.8 occurs about a day earlier in the second drying cycle (Figure 11b) as compared to the first cycle (Figure 10a). An early onset of an equivalent stress condition in the second drying cycle would have been expected because this drying cycle got started with a stressed crop. A spatial variability of irrigation water in addition to the soil hydraulic heterogeniety leads to a little larger spatial variability of canopy temperatures (Fig. 11).

In order to quantify the soil-water induced stress associated with the spatial variation of canopy temperatures, we plotted the CTVs from Figure 11a as a function of PWSI (Figure 12). A CTV = 0.8 corresponds to PWSI between 0.3 and 0.35, which, from Figure 8, give the root-zone soil water potential between −30 and −35 m or a depletion of conventionally defined available water between 65% and 70%. For the soil-plant-atmosphere data used in the present simulation, we are essentially substantiating the long-held wisdom of irrigation scheduling, albeit via the modern technology of infrared remote sensing. (For the CTVs in Figure 11b, however, the crop stress conditions cannot be related unambiguously to the soil water status because of the lag in recovery of canopy temperatures.)

For irrigated corn crops Sumayao et al. (1982) found the leaf stomatal resistances to be less than 500 s m^{-1}, which, according to the present simulation, is consistent with CTV = 0.8 or soil-water potentials between −30 and −35 m (cf., Figures 3 and 5). The field-averaged canopy-air temperature differences are between 2 and 4K when the soil water potentials are between −30 and −35 m.

Our simulations indicate that either a 2-4° canopy-air temperature difference or about 1°C spatial range in canopy temperatures at midday might be suitable indicators of need for irrigation in corn.

REFERENCES

Bartholic, J. F., Namken, L. N. and Wiegand, C. L., 1972. Areal thermal scanner to determine temperature of soils and of crop canopies differing in water stress. Agron. J., 64: 603-608.

Boyer, J. S., 1971. Recovery of photosynthesis in sunflower after a period of low water potential. Plant Physiol., 47: 816-820.

Brady, R. A., Powers, W. L. Stone, L. R. and Goltz, S. M., 1974. Relation of soybean leaf water potential to soil water potential. Agron. J., 66: 795-798.

Campbell, G. S., 1974. A simple method for determining unsaturated conductivity from moisture tension data. Soil Sci., 117: 311-314.

Choudhury, B. J., 1983a. Simulating the effects of weather variables and soil water potential on a corn canopy temperature. Agric. Meteorol. (in press).

Choudhury, B. J., 1983b. Simulation of soybean canopy temperature as affected by rooting density and soil water potential. 16th Conference on Agriculture and Forest Meteorology. Am. Met. Soc., Boston.

Clapp, R. B. and Hornberger, G. M., 1978. Empirical equations for some soil hydraulic properties. Water Resours. Res., 14: 601-604.

Clark, R. N. and Hiler, E. A., 1973. Plant measurements as indicators of crop water deficit. Crop Sci., 13: 466-469.

Clawson, K. L. and Blad, B. L., 1982. Infrared thermometry for scheduling irrigation of corn. Agron. J., 74: 311-316.

Douglas, J. Jr. and Jones, B. F. Jr., 1963. On predictor-corrector methods for nonlinear parabolic differential equations. J. Soc. Indust. Appl. Math., 11: 195-204.

Ehling, C. F., Gardner, W. R. and Clark, M., 1968. Effect of soil salinity on water potential and transpiration in pepper. Agron. J., 60: 249-253.

Feddes, R. A. and Rijtema, P. E., 1972. Water withdrawal by plant roots. J. Hydrol., 17: 33-59.

Federer, C. A., 1979. A soil-plant-atmosphere model for transpiration and availability of soil water. Water Resour. Res., 15: 555-562.

Grace, J., 1977. Plant Response to Wind. Academic Press. New York.

Idso, S. B., 1981. A set of equations for full spectrum and 8- to 14-μm and 10.5- to 12.5-μm thermal radiation from cloudless skies. Water Resour. Res., 17: 295-304

Idso, S. B., 1982. Non-water-stressed baselines: A key to measuring and interpreting plant water stress. Agric. Meteorol. (in press).

Idso, S. B., Jackson, R. D., Printer, P. J. Jr., Reginato, R. J. and Hatfield, J. L., 1981. Normalizing the stress-degree-day parameter for environmental variability. Agric. Meteorol., 24: 45-55.

Impens, I. and Lemeur, R., 1969. Extinction of net radiation in different crop canopies. Arch. Met. Geoph. Biokl., B17: 403-412.

Jackson, R. D., 1982. Canopy temperature and crop water stress in Advances in Irrigation, Vol. 1 (ed., D. Hillel), Academic Press. New York.

Jackson, R. D., Reginato, R. J. and Idso, S. B., 1977. Wheat canopy temperature: A practical tool for evaluating water requirements. Water Resour. Res., 13: 651-656.

Jackson, R. D., Idso, S. B., Reginato, R. J. and Pinter, P. J. Jr., 1981. Canopy temperature as a crop water indicator. Water Resour. Res., 17: 1133-1138.

Kramer, P. J., 1969. Plant and water relationships: A modern synthesis. McGraw-Hill, New York.

Milne, R., Ford, E. D. and Deans, J. D., 1983. Time lags in the water relations of Sitka spruce. For. Ecol. Mgt., 5: 1-25.

Monteith, J. L., 1965. Evaporation and environment. The State and Movement of Water in Living Organisms (ed. G. E. Fogg), p. 205-234. Academic Press. New York.

Monteith, J. L. 1981. Evaporation and surface temperature. Quart. J. R. Met. Sco., 107: 1-27.

Newman, E. K., 1973. Permeability to water of the roots of five herbaceous species. Net Phytol., 72: 547-555.

Nulsen, R. A. and Thurtell, G. W., 1978. Recovery of corn leaf water potential after severe water stress. Agron. J., 70: 903-906.

Philip, J. R., 1980. Field heterogeneity: Some basic issues. Water Resour. Res., 16: 443-448.

Reicosky, D. C., Campbell, R. G. and Doty, C. W., 1975. Diurnal fluctuation of leaf-water potential of corn as influenced by soil matrix potential and microclimate. Agron. J., 65: 380-385.

Reicosky, D. C. and Lambert, J. R., 1978. Field measured and simulated corn leaf water potential. Soil Sci. Soc. Am. J., 42: 221-228.

Reicosky, D. C. and Ritchie, J. T., 1976. Relative importance of soil resistance and plant resistance in root water absorption. Soil Sci. Soc. Am., 40: 293-297.

Schmer, F. A. and Werner, H. D., 1974. Remote sensing techniques for evaluation of soil water conditions. Trans. Am. Soc. Agr. Engr., 17: 310-314.

Shinn, J. H. and Lemon, E. R., 1968. Photosynthesis under field conditions. XI. Soil-plant-water relations during drought stress in corn. Agron. J., 60: 337-343.

Sumayao, C. R., Kanemasu, E. T. and Brakke, T. W., 1980. Using leaf temperature to assess evapotranspiration and advection. Agric. Meteorol., 22: 153-166.

Tanner, C. B., 1963. Plant temperatures. Agron. J., 55: 210-211.

Uchijima, Z., 1976. Maize and rice. p. 33-34. Vegetation and the Atmosphere. Vol. 2 (J. L. Monteith, ed.) Academic Press. New York.

Vaadia, Y., Raney, F. C. and Hagan, R. M., 1961. Plant water deficits and physiological processes. Annu. Rev. Plant Physiol., 12: 265-292.

van den Honert, T. H., 1948. Water transport as a catenary process. Discuss. Faraday Soc., 3: 146-153.

Wang, J., O'Neill, P., Engman, E., McMurtrey, J., III, Lawless, P., Schmugge, T., Jackson, T., Gould, W., Fuchs, J. and Glazer, W., 1982. Remote measurements of soil moisture by microwave radiometers at BARC test site, II. NASA-TM-83954. Goddard Space Flight Center, Maryland.

Warrick, A. W., Mullen, G. J. and Nielsen, D. R., 1977. Scaling field-measured soil hydraulic properties using a similar media concept. Water Resour. Res., 13: 355-362.

CAPTION TO THE FIGURES

Figure 1. Relationship of plant storage water potential and plant water content. See text for the meaning of symbols.

Figure 2. Observed microclimatic data, and observed and simulated leaf water potentials. The data in (2a) and (2c) are from Reicosky et al. (1975), and (2b) from Reicosky and Lambert (1978).

Figure 3. Simulated canopy-air temperature difference and soil water potential at 1300 hour of different days. A simulated irrigation is done at 0100 hour of the 11th day. The air temperature is constant for each data set, so variation in the canopy-air temperature difference is caused by variation in canopy temperature.

Figure 4. Dirunal variation of canopy-air temperature difference. The curves are labeled by the day of simulation as shown in Fig. 3.

Figure 5. Leaf water potential and leaf stomatal resistance at 1300 hour of various days of simulation. Note the lag in recovery after irrigation at 0100 hour on the eleventh day.

Figure 6. Relationships of 1300 hour leaf and soil water potentials for the three data sets.

Figure 7. Relationships of 1300 hour leaf water potential and canopy-air temperature difference for the three data sets.

Figure 8. Relationship of 1300 hour plant water stress index as defined by equation (31) and soil water potential.

Figure 9. Relationships of 1300 hour plant water stress index and crop water stress index.

Figure 10. Relationships of daily total transpiration and 1300 hour canopy-air temperature difference.

Figure 11. The range of canopy temperatures at 1300 hour for the three data sets. (a) the variability originating from spatial variation of soil hydraulic properties, (b) the variability originating from spatial variation of soil hydraulic properties and irrigation water application.

Figure 12. Relationships of 1300 hour plant water stress index and spatial variability of canopy temperatures resulting from soil hydraulic heterogeniety.

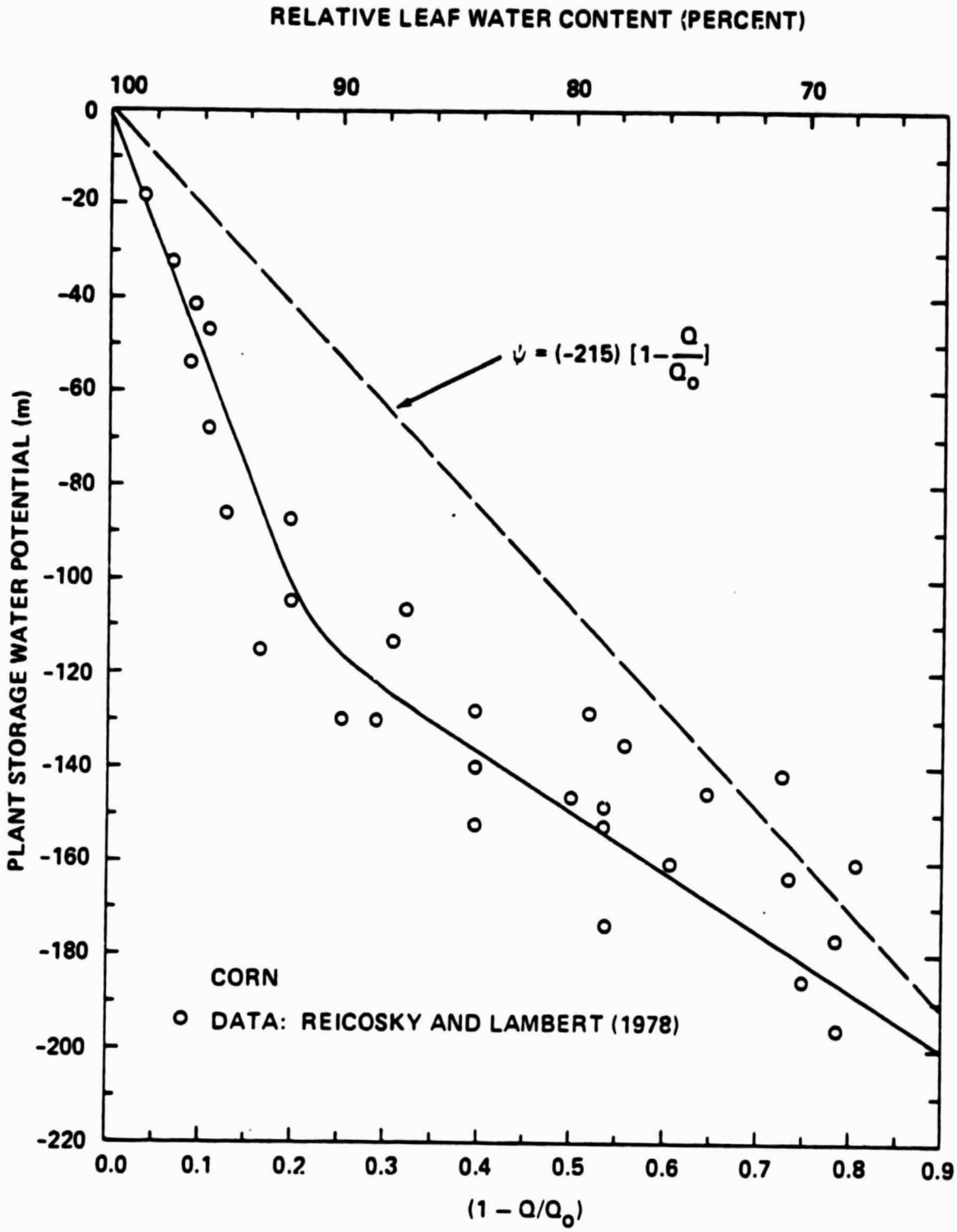

Figure 1

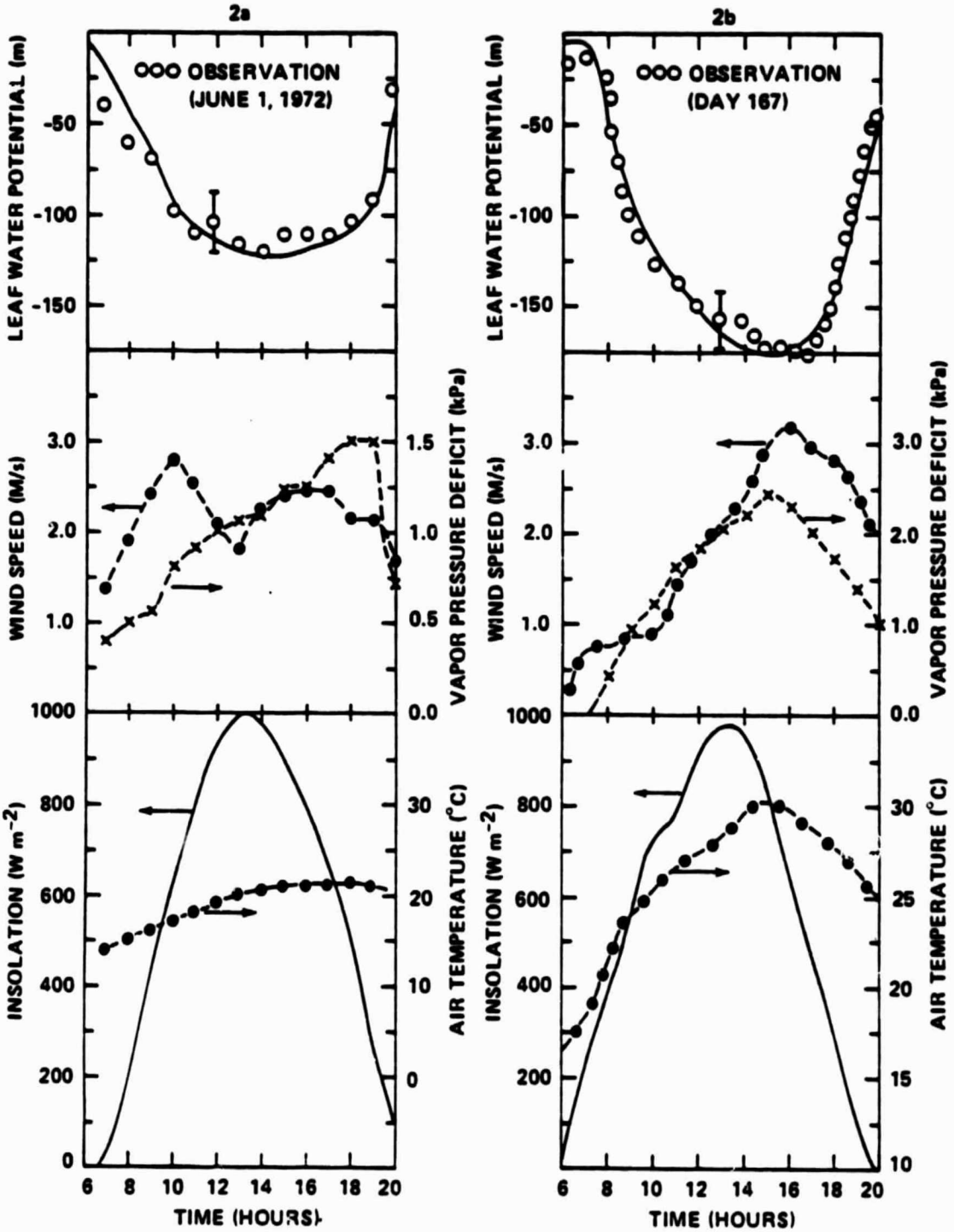

Figure 2

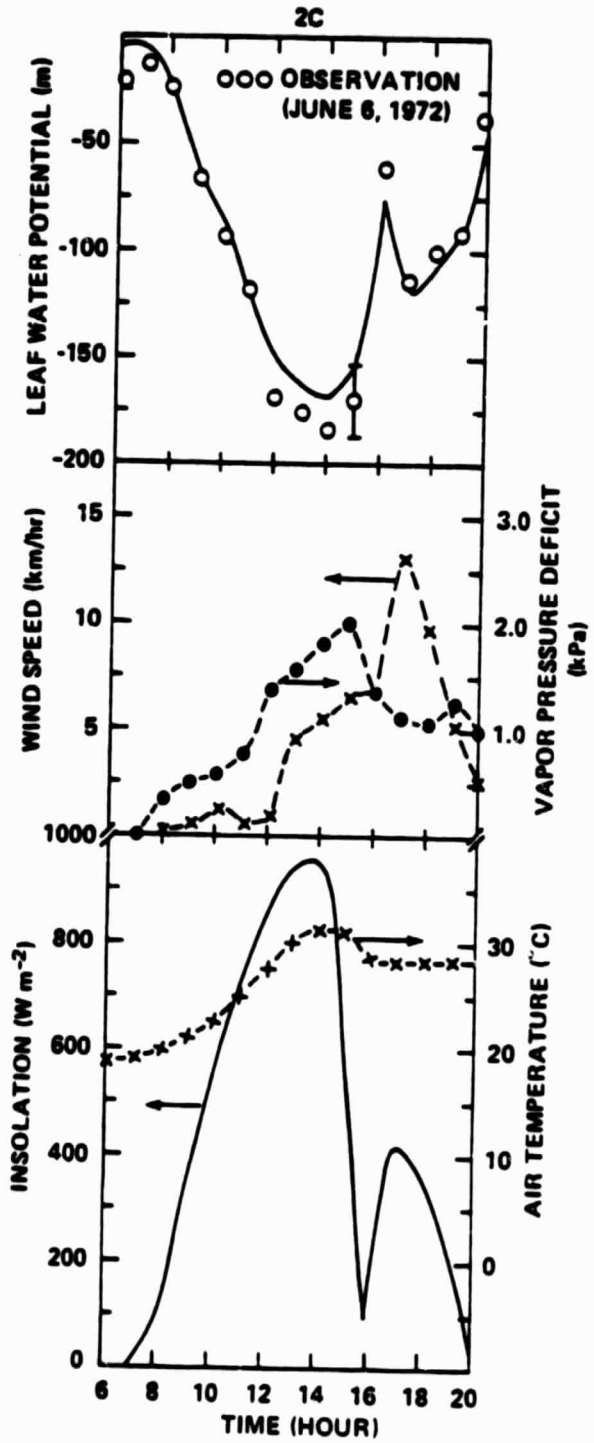

Figure 2

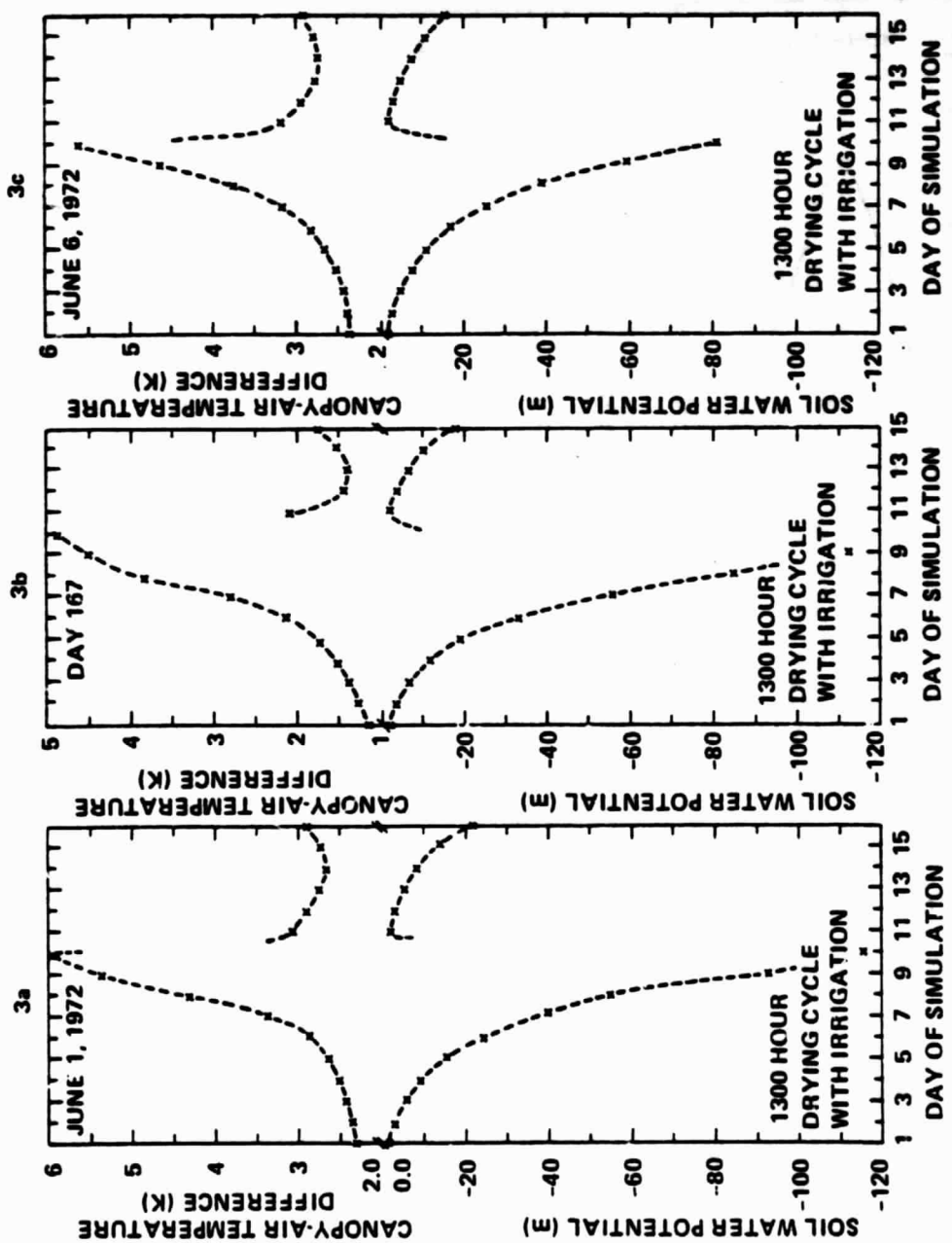

Figure 3

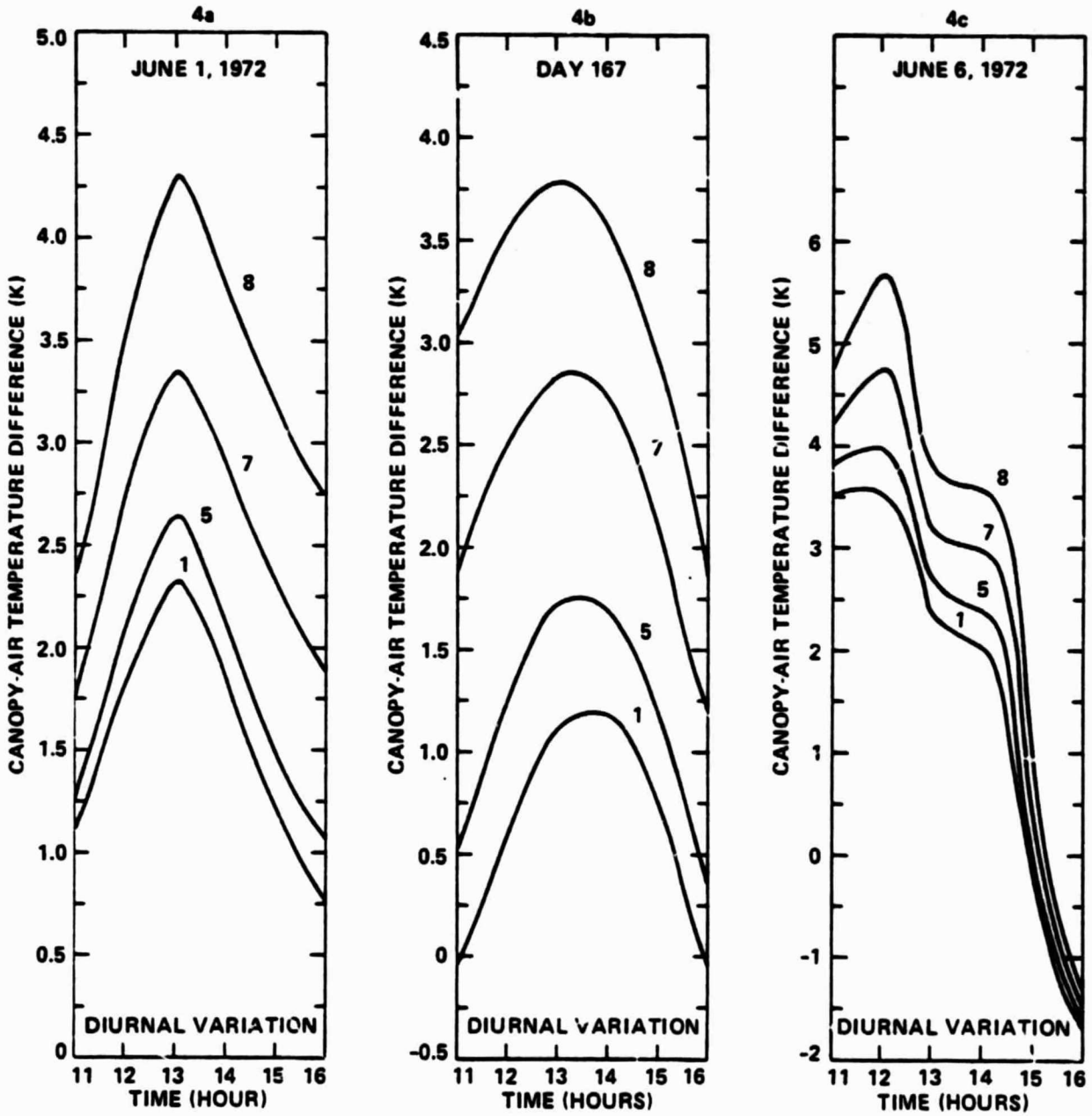

Figure 4

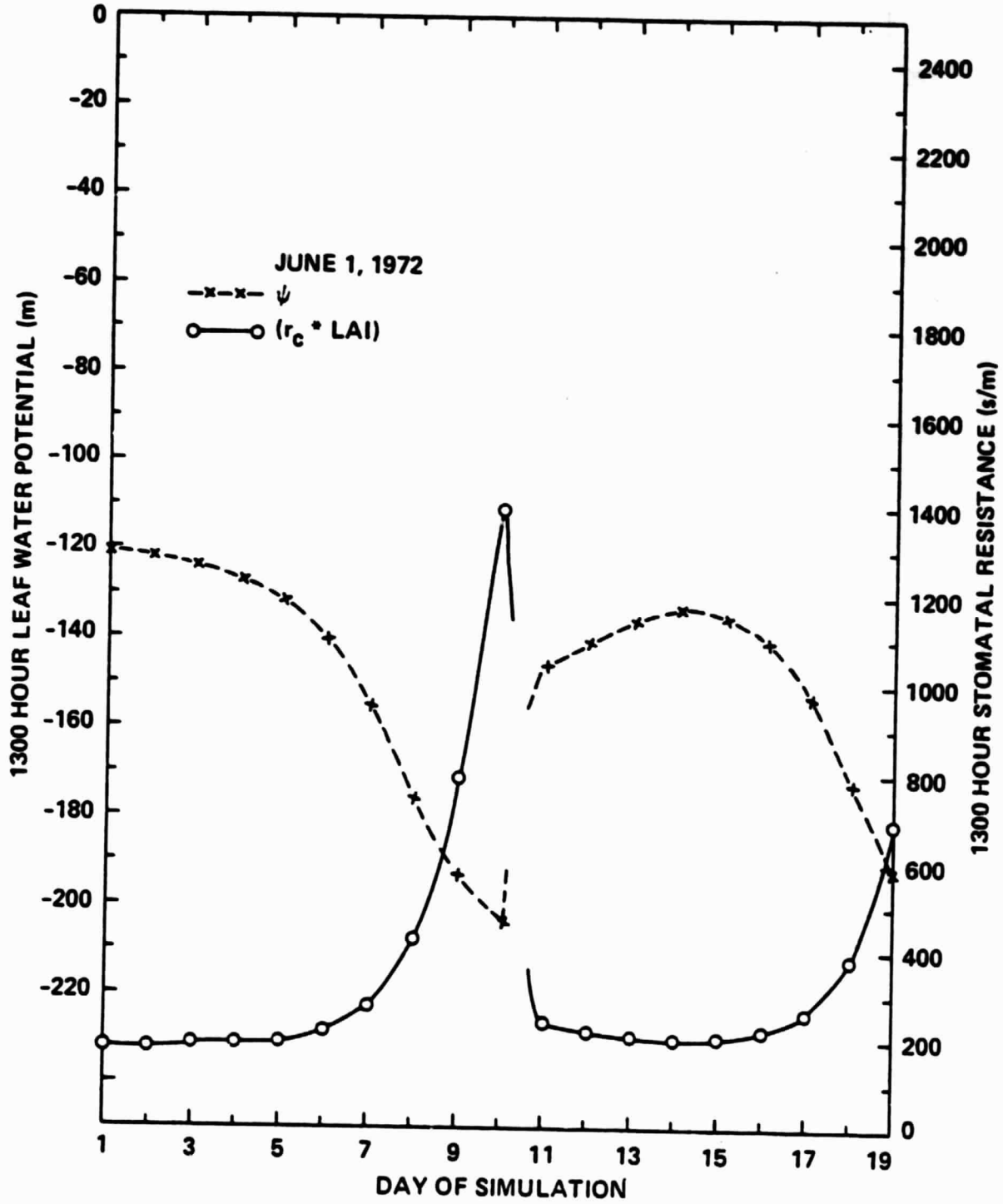

Figure 5a

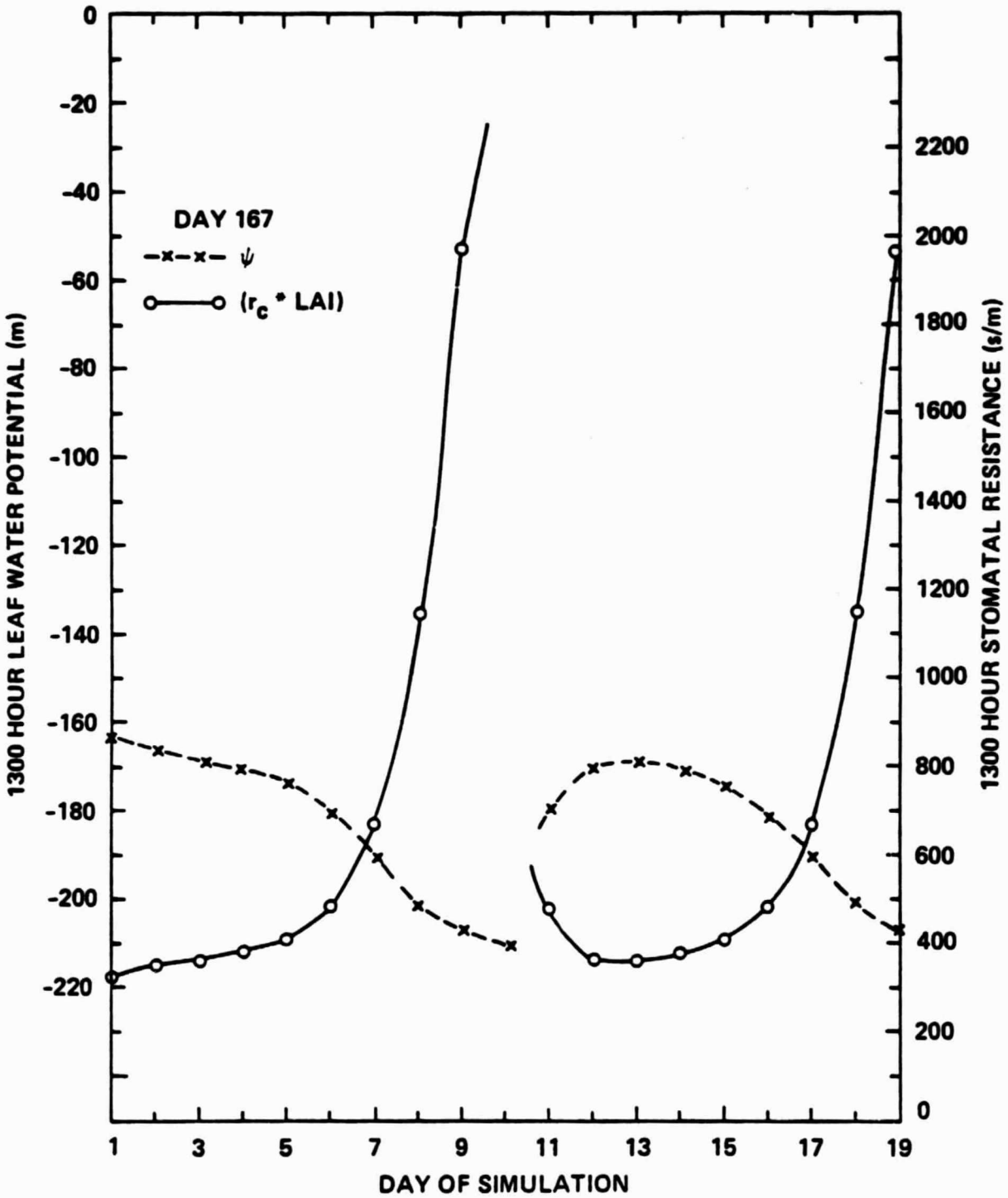

Figure 5b

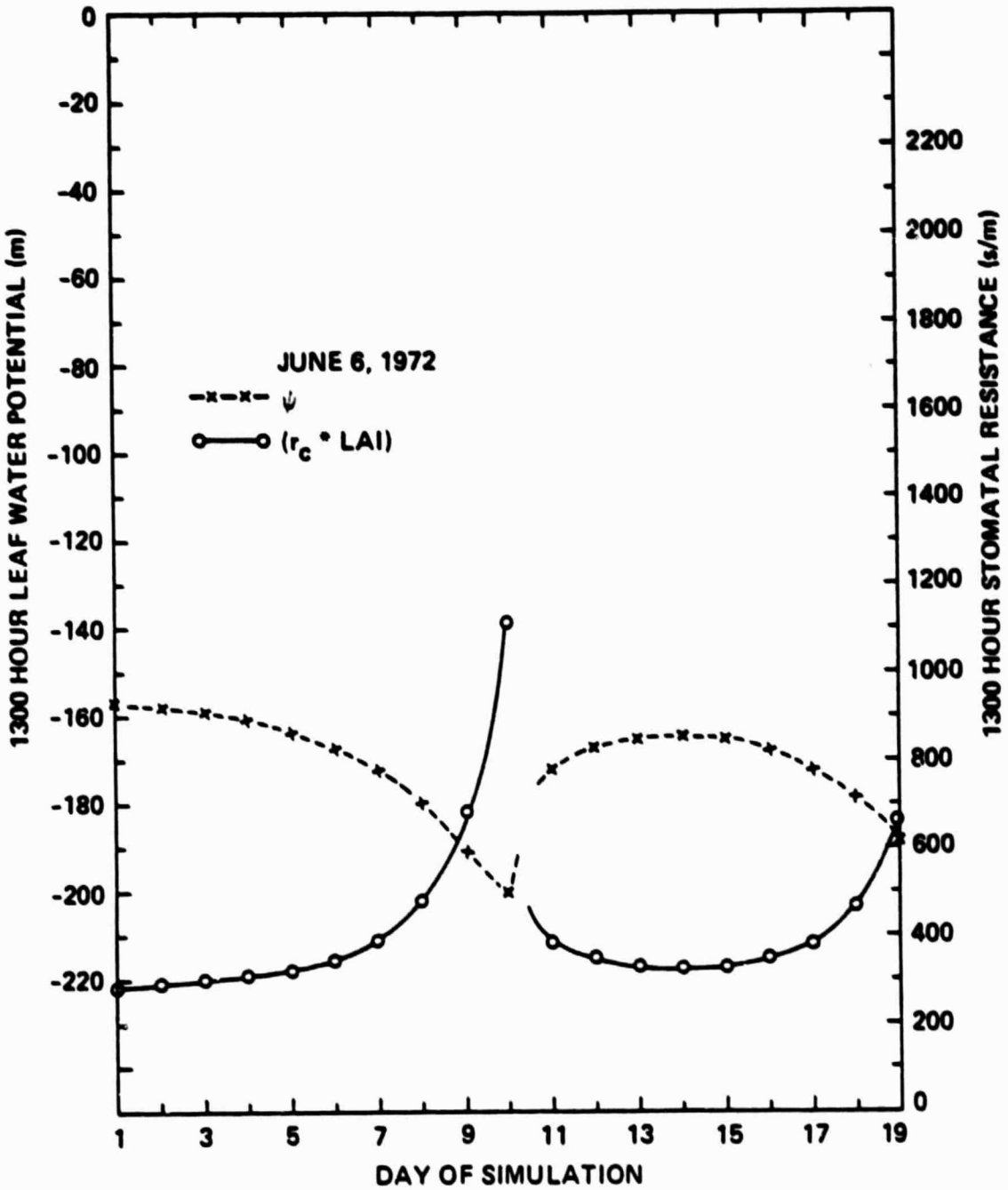

Figure 5c

ORIGINAL PAGE IS
OF POOR QUALITY

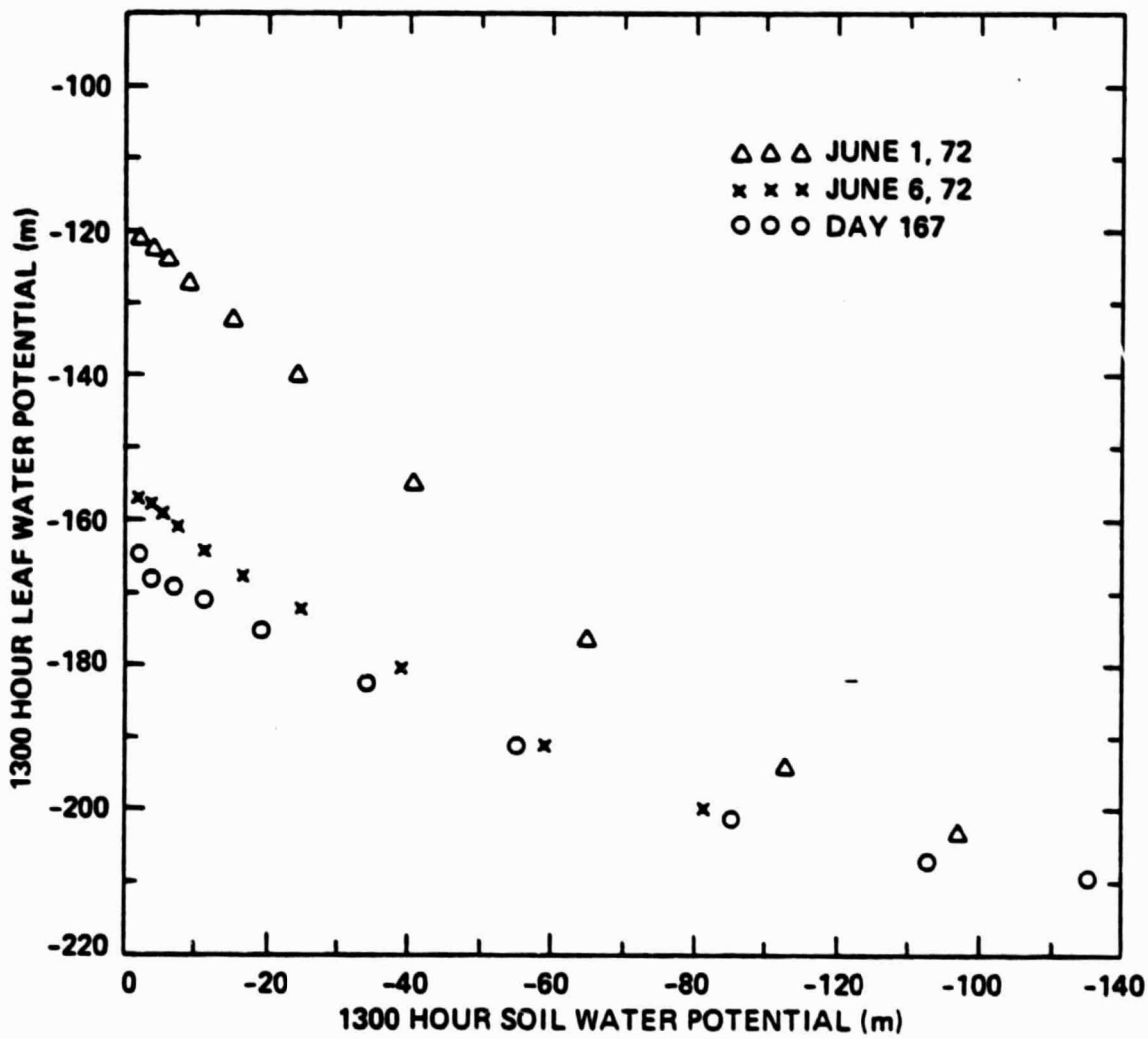

Figure 6

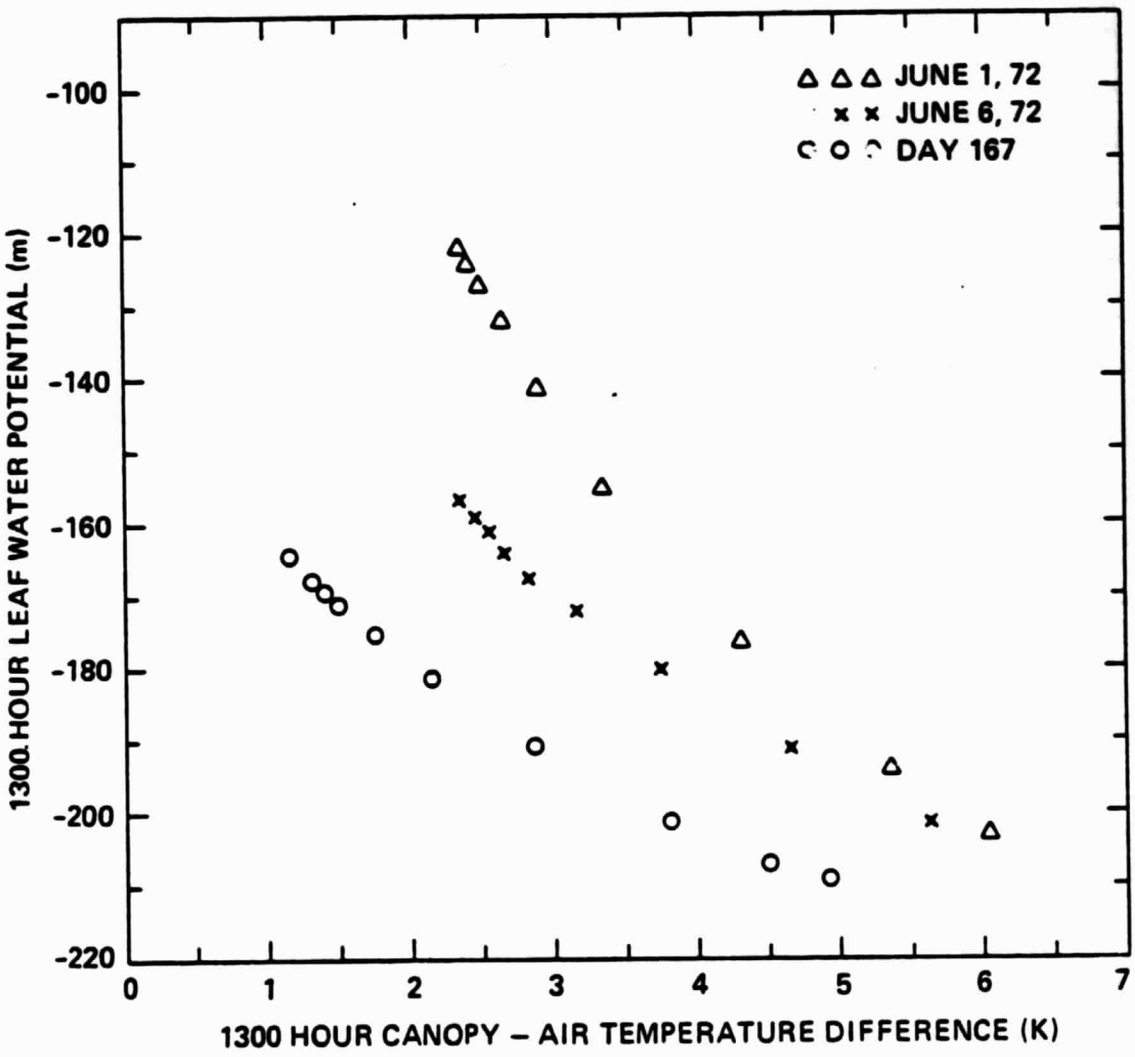

Figure 7

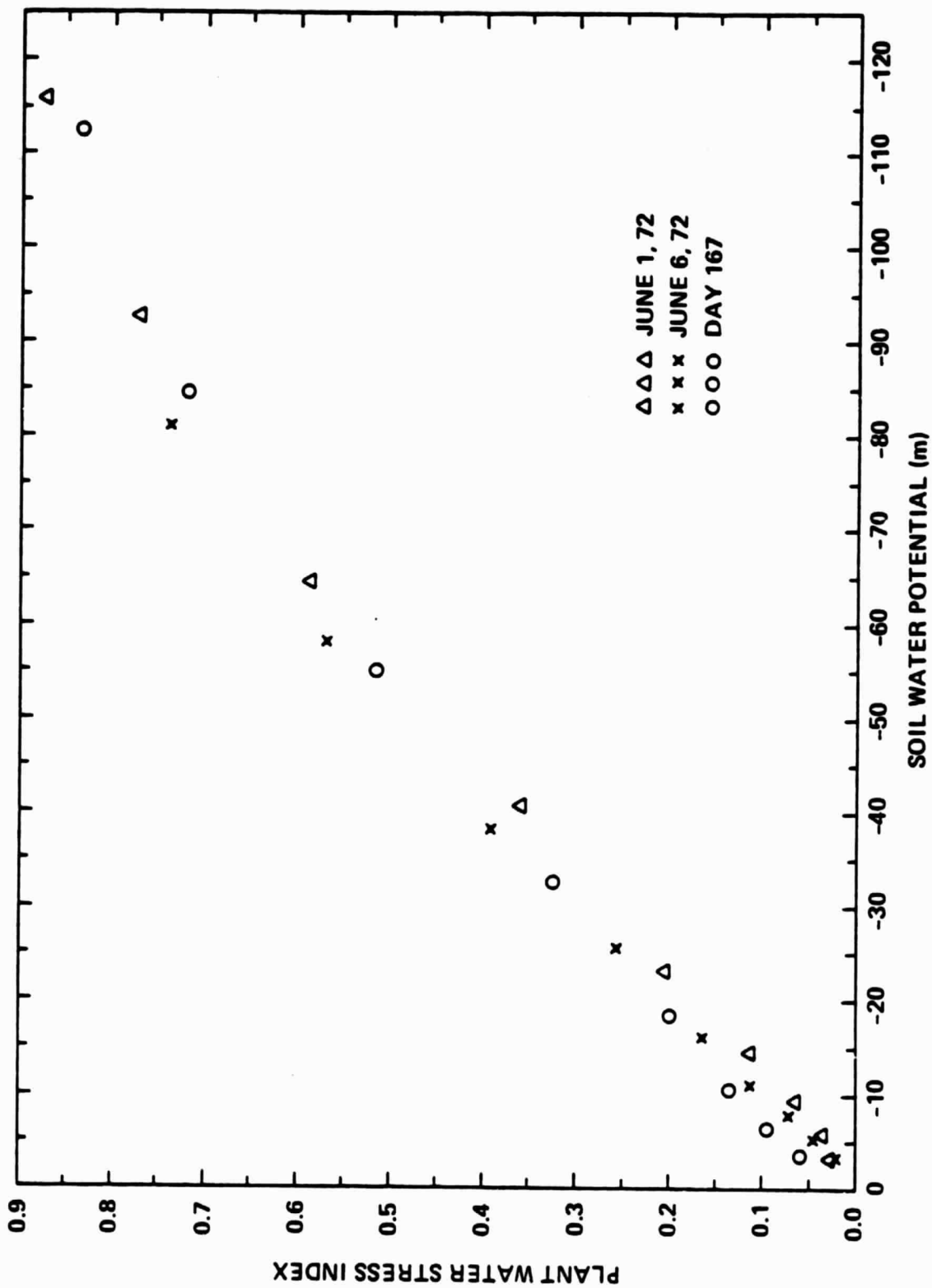

Figure 8

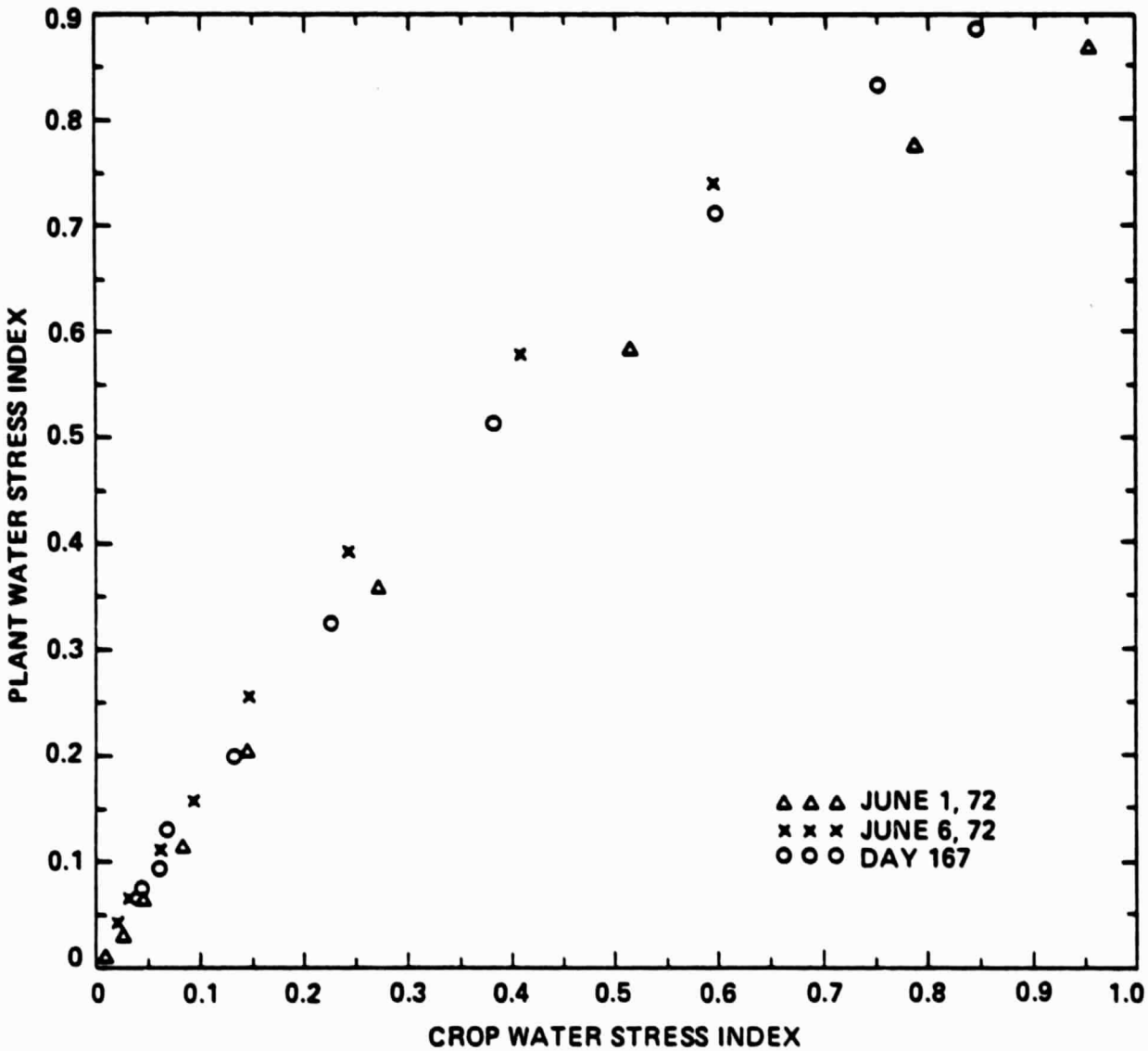

Figure 9

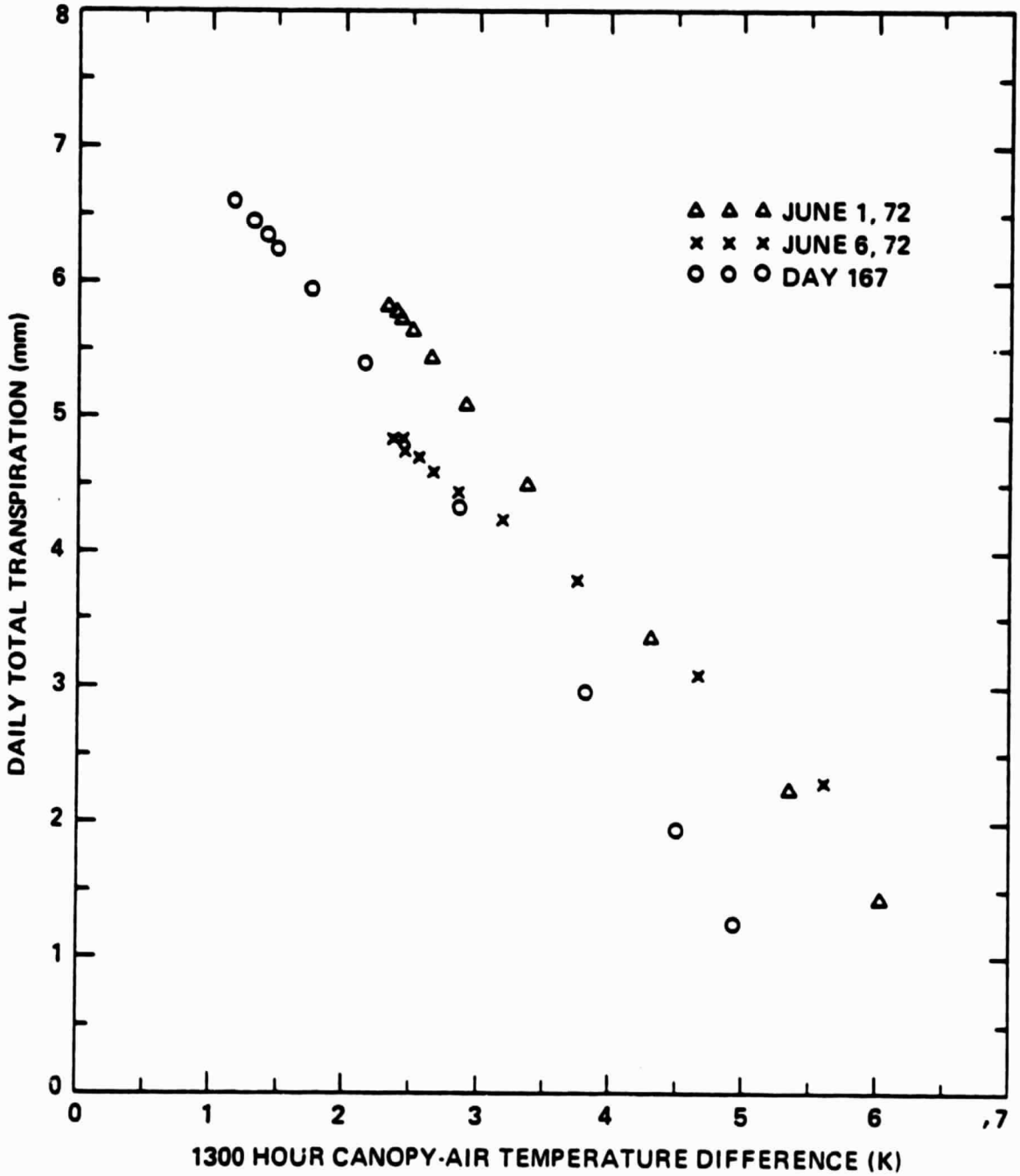

Figure 10

ORIGINAL PAGE IS
OF POOR QUALITY

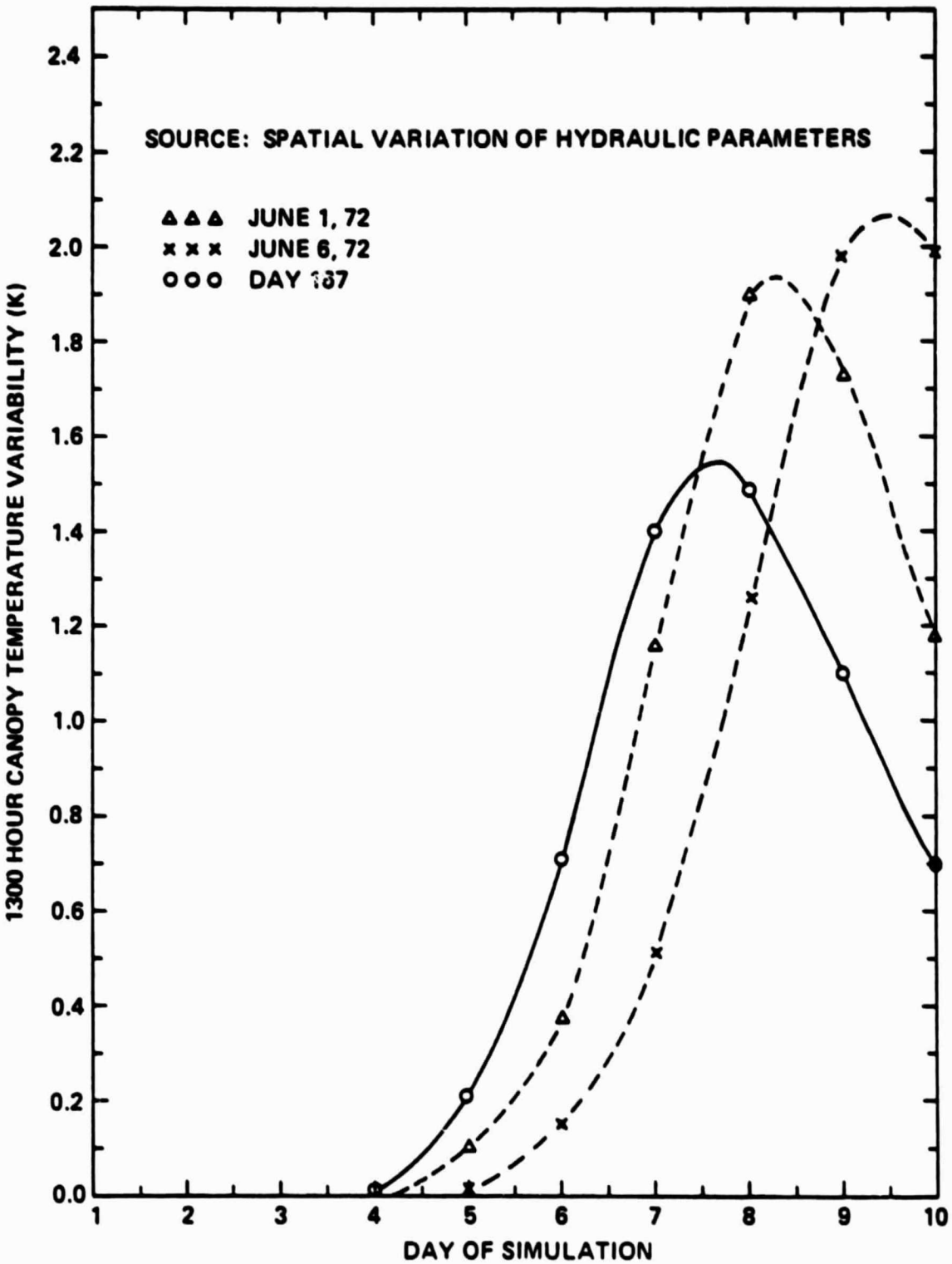

Figure 11a

ORIGINAL PAGE IS
OF POOR QUALITY

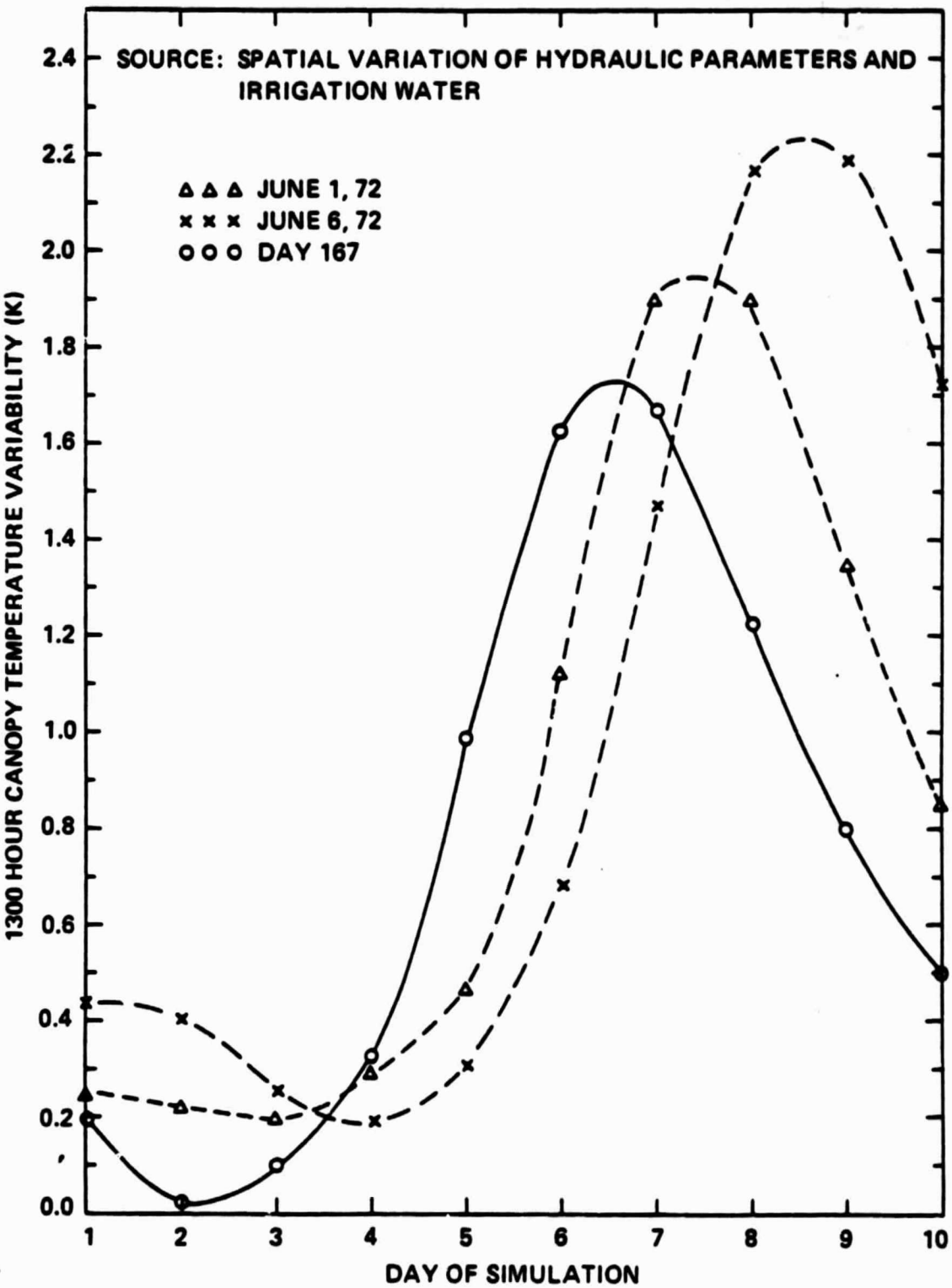

Figure 11b

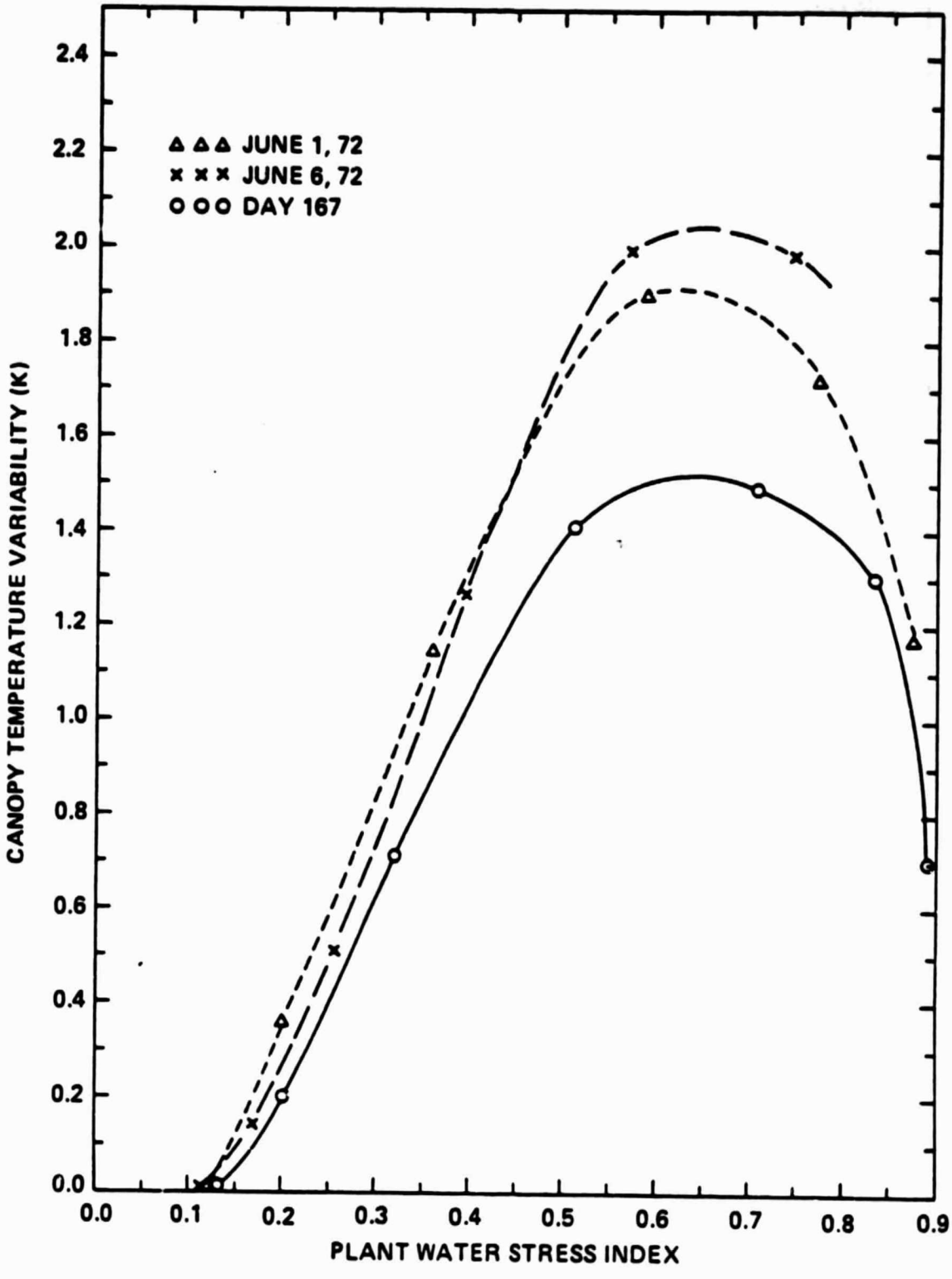

Figure 12